



# Electric arc synthesis of magnetic Mn-Fe-C nanoparticles

D. V. Smovzh<sup>†,1,2</sup>, M. S. Skirda<sup>1</sup>, S. Z. Sakhapov<sup>1</sup>

<sup>†</sup>smovzh@itp.nsc.ru

<sup>1</sup>Institute of Thermophysics n. a. S. S. Kutateladze SB RAS, Novosibirsk, 630090, Russia

<sup>2</sup>Novosibirsk State University, Novosibirsk, 630090, Russia

The aim of this research is to investigate the phase transformations and magnetic properties of nanoparticles formed during electric arc sputtering of composite Fe-Mn-C with subsequent annealing of the resulting composite in an oxygen atmosphere. As a result of the study, pure metals, mixed oxides, carbides, and carbon nanocomposites are synthesized. The magnetic susceptibility of Fe-Mn-C composites grows with an annealing temperature increase up to 600°C as compared to the iron-carbon system. The obtained methods and results can serve as a base for new synthesis techniques to obtain composite magnetic nanoparticles with a low carbon content.

**Keywords:** magnetic nanoparticles, carbon arc discharge, spinel ferrites.

## 1. Introduction

With the active development of nanotechnologies, the direction associated with the synthesis of magnetic nanoparticles is intensively developing. There are numerous applications for nanoparticles in chemical, biological, and medical fields. Magnetic nanoparticles (MNPs) can intensify heat and mass transfer processes in liquid and gaseous media [1]. With MNPs it is possible to transport materials via liquids through various channels and porous media to perform targeted drug delivery, as well as to intensify flows through porous media [2–5]. The properties of MNPs substantially depend on their geometric and structural parameters. Based on the study [6], iron oxide particles with decreasing sizes have a lower saturation magnetization. The authors also stated that with the size reduction the surface area increases, which could affect the non-crystalline characteristics of MNPs and hence, their magnetic moments. The tiniest MNPs can exhibit superparamagnetic properties demonstrating better magnetization compared to paramagnetic materials [7]. Generally, magnetic properties of MNPs are determined by the crystallinity and purity of their constituent minerals.

The size distribution function and subsequent functionalization parameters of the surface of MNPs determine their physicochemical properties, stability, and mobility [6]. At present, methods are being developed for the synthesis of MNPs, which enable precise control of their parameters. One can divide these methods into physical, chemical, and biological or microbial methods [8]. Physical methods include top-down approaches, such as the bulk materials shredding and physical gas-phase sputtering technologies [9–12]. Chemical methods include chemical vapor deposition technologies, solution chemistry technologies, aerosol methods [13–16], etc. The biological methods rely on the fact that cells and microorganisms synthesize and accumulate magnetic nanoparticles throughout their life cycles [17,18].

Regarding the differences between these methods, one should note here that the chemical methods have an

advantage over the others in their flexibility regarding the feedstock and a wide variation in methods. Physical methods give less freedom to control the process but eliminate the need to use aggressive chemicals, which often require disposal and remain in the products as chemical contaminants. Even though biological technologies are cheap in energy and environmental terms, they are poorly scalable and do not allow varying product parameters over a wide range.

Arc discharge synthesis of nanocomposites with the use of graphite rods is one of the representatives of physical methods that can be used to synthesize a wide class of composite compounds. The main advantage of arc discharge synthesis is the ability to control the shape and size and composition of nanoparticles. In [19,20], iron nanoparticles in a carbon matrix were obtained by electric arc discharge and their magnetic properties were studied. It has been shown that nanoparticles are superparamagnetic, and their magnetic properties and composition substantially depend on the subsequent heat treatment after synthesis.

Magnetic nanoparticles can have different structures, such as core-shell, shell-core-shell structure, and Janus particle structure [2]. The formation of core-shell particles is possible in various ways [21]. In an arc discharge, such particles can be formed during the simultaneous sputtering of materials with different saturated vapor pressures. The components condense at different temperatures, or during the oxidation of the surface of nanoparticles upon contact with the external atmosphere and form core-shell particles [22]. One of the challenges is the synthesis of composite magnetic nanoparticles consisting of a magnetic material and a functional additive. The magnetic component in such a composite allows one to manipulate a particle in a magnetic field, and the additive can be a catalyst for a chemical reaction, an abrasive for surface polishing, a drug, etc. The purpose of this work is to study composite Fe-Mn nanoparticles obtained by arc discharge in a carbon matrix, and to analyze changes in their properties during the heat treatment.

## 2. Materials and experimental methods

Electric arc sputtering of the materials was carried out in a vacuum chamber (Fig. 1) in a helium atmosphere using a direct current source. The sputtered graphite electrodes had a diameter of 8 mm. A mixture of powders (100  $\mu\text{m}$ ) Fe:Mn:C was pressed into the anode hole with a diameter of 4.2 mm in a mass ratio of 7:3:30. Sputtering was carried out at a discharge current of 100 A and a voltage of 20 V. The electrode was sputtered for 17 min at a rate of 0.2 g of material per minute, which corresponds to an energy consumption of the process of 0.17 kW/g. Then the material was collected from the cooled walls of the reactor. Annealing of the samples was carried out in the air atmosphere at temperatures of 100–1000°C, with a step of 50°C, the holding time at each temperature was 1 hour. Obtained materials were analyzed using JEOL JEM-2200FS CS electron microscopy and X-ray diffraction (XRD) analysis on a Bruker D8. The magnetic susceptibility of the material was measured with the SM150L, in a magnetic field of 320 A/m, at frequency range of 63–16 000 Hz.

## 3. Results and discussion

Analysis of Fe-Mn-C materials by transmission electron microscopy showed that the material after arc discharge sputtering consists of nanoparticles embedded in the carbon matrix, Fig. 2. According to the diffraction patterns obtained

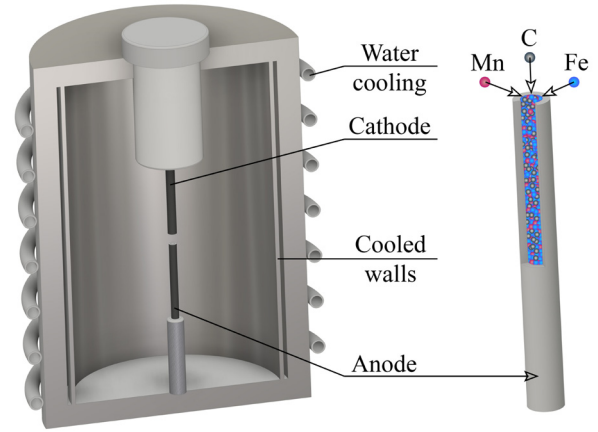


Fig. 1. (Color online) Experimental setup.

Table 1. Normalized magnetic susceptibility of materials.

Materials	$\chi/\chi_{\text{Fe}}$
Fe	1.00
Mn	0.03
Fe <sub>3</sub> C	0.61
Mn <sub>x</sub> Fe <sub>3-x</sub> O <sub>4</sub>	0.01–1.00
$\gamma$ -Fe <sub>2</sub> O <sub>3</sub>	0.46
$\alpha$ -Fe <sub>2</sub> O <sub>3</sub>	0.00
Fe <sub>3</sub> O <sub>4</sub>	0.46
Mn <sub>2</sub> O <sub>3</sub>	0.70

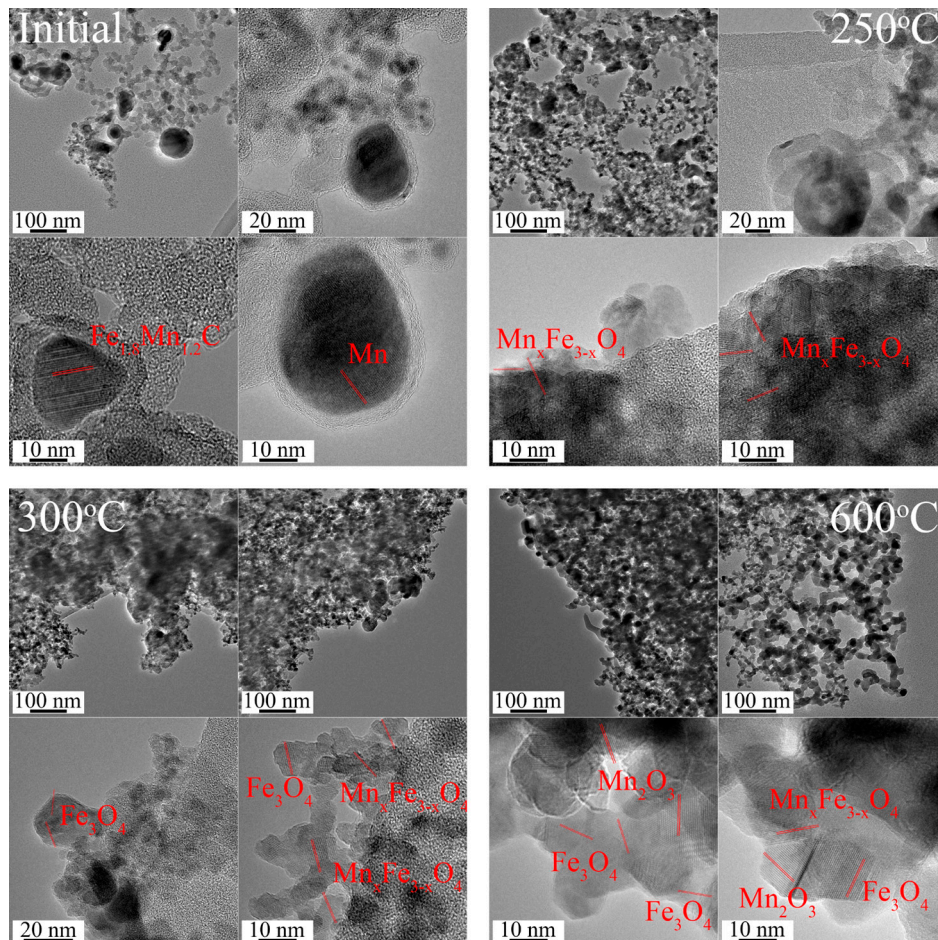


Fig. 2. TEM image of Fe-Mn-C initial and annealed at different temperatures.

from individual nanoparticles, the initial composition corresponds to metals, their carbides and alloys; however, it is difficult to resolve individual lattices due to their similar parameters. Annealing at a temperature of 250°C leads to the formation of nanoparticles of manganese and iron oxides and their mixtures. With an increase in the annealing temperature, the formation of nanoparticles of the mixed oxide  $\text{Mn}_x\text{Fe}_{3-x}\text{O}_4$  with a higher magnetic susceptibility (Table 1) occurs. During subsequent annealing (300–600°C), the stoichiometry of  $\text{Mn}_x\text{Fe}_{3-x}\text{O}_4$  nanoparticles changes, which can lead to a change in their magnetic properties [23]. At high annealing temperatures, the nanoparticles are completely oxidized to iron oxide  $\text{Fe}_3\text{O}_4$  and  $\text{Mn}_2\text{O}_3$ , Fig. 2.

Figure 3a presents the dependence of the magnetic properties of the Fe-Mn-C composite on the calcination temperature. Figure 3b shows how the magnetic susceptibility depends on the calcination temperature for the Fe-C composite. The magnetic susceptibility of the iron-carbon composite sharply decreases upon annealing at a temperature of 200°C, as in work [20]. It is associated with the oxidation of iron and iron carbide nanoparticles. Further, the material magnetic properties deteriorate due to the phase transition of iron oxide from  $\gamma\text{-Fe}_2\text{O}_3$  to  $\alpha\text{-Fe}_2\text{O}_3$  at calcination temperatures above 600°C [20].

According to XRD data for pure materials Fe-C [20] and Mn-C [24], the resulting composites consist of carbide  $\text{Fe}_3\text{C}$  and iron nanoparticles mixtures in a carbon matrix for Fe-C and oxide MnO and carbide  $\text{Mn}_7\text{C}_3$  for the Mn-C composite. Nanoparticles of iron and iron carbide have pronounced ferromagnetic properties (Table 1), which leads to the fact that the original composite shows high magnetic susceptibility values. According to the XRD data in Fig. 4, nanoparticles of pure manganese, iron, and carbide with  $\text{Fe}_{1.8}\text{Mn}_{1.2}\text{C}$  stoichiometry form during the combined sputtering of the composite. Composite annealing leads to the disappearance of manganese particles and the formation of Mn-Fe-O alloys with a higher manganese content than in the original carbide. Annealing at a temperature of more than 600°C leads to the formation of manganese oxides  $\text{Mn}_2\text{O}_3$  and iron oxides  $\text{Fe}_3\text{O}_4$ , Fig. 4.

One of the most popular and promising applications of magnetic nanoparticles is currently associated with their use as contrast agents in magnetic resonance spectroscopy. The main materials for such applications are magnetite ( $\text{Fe}_3\text{O}_4$ ) and maghemite  $\gamma\text{-Fe}_2\text{O}_3$ ; the nanoparticles characteristic size varies from 10 to 100 nm [25]. These nanoparticles are obtained by solution chemistry methods, mainly by the thermal decomposition of salts. It is necessary to use various surfactants to stabilize the nanoparticles and ensure their biocompatibility, and protect nanoparticles from coagulation in these methods. The mass fraction of the protective shell in a nanoparticle can reach up to 90% [25], which affects the composite magnetic efficiency. The search for ways to improve the magnetic properties of the obtained nanoparticles is one of the urgent modern problems. One of the strategies for enhancing the magnetic properties of nanoparticles is to dope ferrite with ferromagnetic elements such as manganese (Mn), cobalt (Co), or nickel (Ni) [26]. Among such doped composites, the Mn-Fe composite shows the best properties. Studies of the magnetic properties of  $\text{Mn}_x\text{Fe}_{3-x}\text{O}_4$

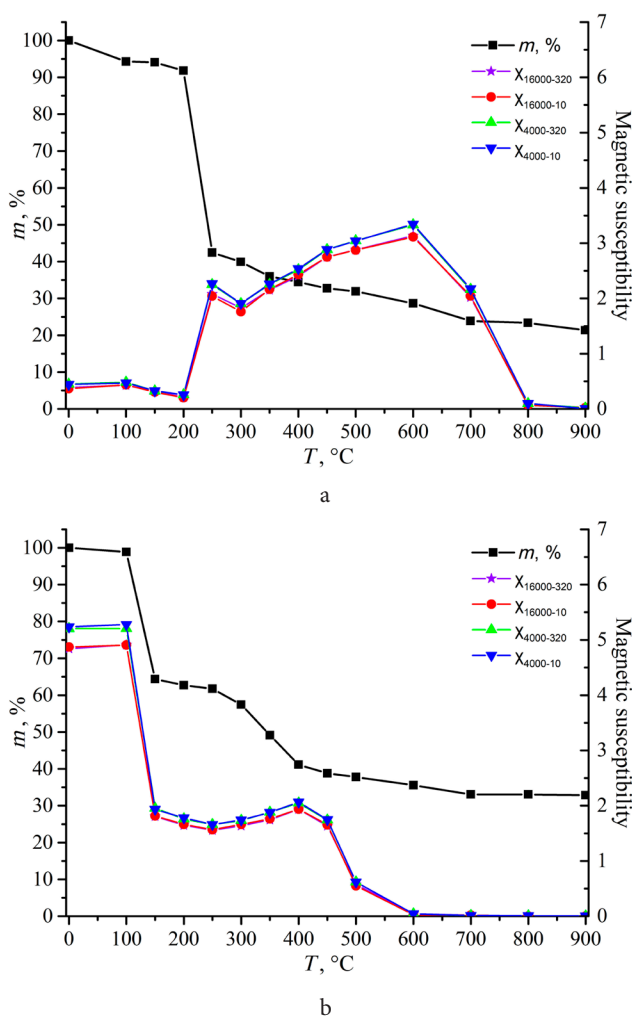


Fig. 3. (Color online) Magnetic susceptibility at various annealing temperatures, Fe-Mn-C (a), Fe-C (b).

are presented in [25,27]. According to these papers, the maximum magnetization is achieved for  $\text{MnFe}_2\text{O}_4$ . The magnetic nanoparticles synthesis technique is based on the thermal decomposition of metal complex precursors (iron pentacarbonyl, iron cupferron, iron tris (2,4-pentadionate)) in an organic solution containing surfactants (fatty acids and amine surfactants). Precursor thermal decomposition leads to the formation of monomers, the aggregation of which, upon supersaturation of the solution, leads to nucleation and growth of nanoparticles [28]. The parameters of synthesized nanoparticles are controlled by varying the monomer concentration, growth time, temperature, and choosing a solvent and surfactants. Despite the high selectivity concerning the synthesis of monodisperse nanoparticles, the problems of these methods include the need to select a precursor, solution, and surfactant with thermal properties suitable for synthesis, which significantly limits the range of synthesis products. In addition, solution chemistry methods use intermediate reagents that require complex disposal, and products tend to contain residues of intermediate substances, which physical methods usually lack.

The analysis of materials obtained in the course of synthesis in an electric arc discharge of the Mn-Fe-C complex presented in this article showed that during sputtering

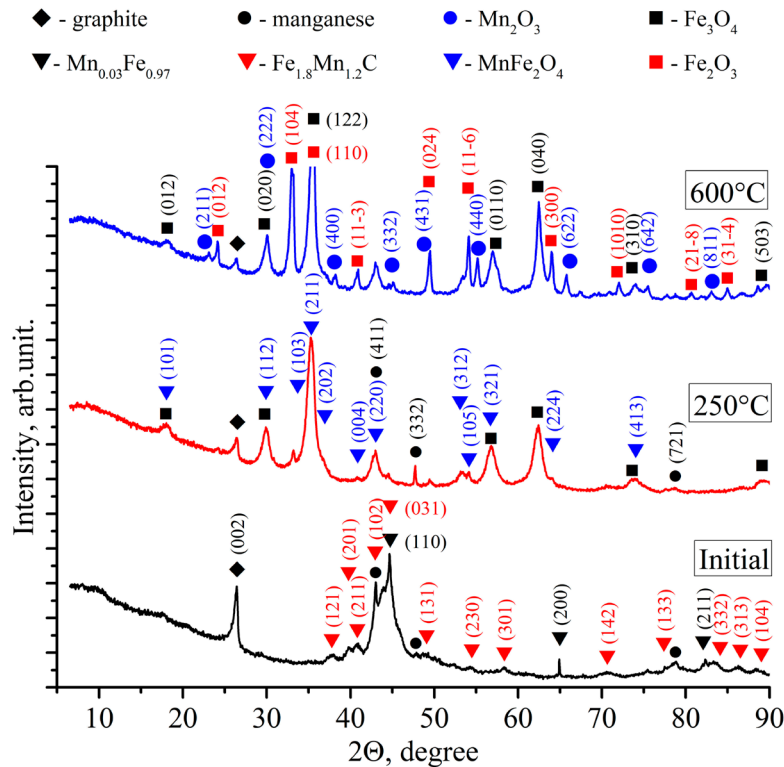


Fig. 4. (Color online) XRD of Fe-Mn-C initial and annealed at different temperatures.

and annealing of the material, magnetic  $\text{Mn}_x\text{Fe}_{3-x}\text{O}_4$  nanoparticles with a size of about 10 nm are formed, which corresponds to the products obtained by the methods of solution chemistry presented in scientific literature. Under the conditions of electric arc discharge, the stoichiometry and size of nanoparticles can vary over a wide range, which significantly expands the opportunities for the magnetic nanoparticles synthesis. The resulting magnetic nanoparticles have high thermal stability: heating to 600°C does not lead to coagulation and degradation of magnetic properties.

Thus, the electric arc discharge can be used to synthesize magnetic nanoparticles based on  $\text{Mn}_x\text{Fe}_{3-x}\text{O}_4$  alloys, manganese, and iron oxides. In this case, the products of synthesis with subsequent calcination change significantly, in contrast to pure Mn-C and Fe-C systems. The presence of manganese vapor in the arc discharge atmosphere leads to the formation of mixed  $\text{MnFeC}$  carbide and pure manganese and iron nanoparticles. Annealing the resulting composites in the temperature range of 250–600°C leads to the material magnetic susceptibility increase due to the formation of  $\text{Mn}_x\text{Fe}_{3-x}\text{O}_4$  nanoparticles and subsequent changes in their stoichiometry. After annealing at 600°C the composite magnetic properties are determined by  $\text{Mn}_2\text{O}_3$  nanoparticles. In Fig. 2 (600°C), we can observe a crystal lattice of manganese oxide  $\text{Mn}_2\text{O}_3$  and iron  $\text{Fe}_3\text{O}_4$ , as well as a region of transition from one lattice to another. The formation of such polycrystalline particles is associated with the thermal decomposition of the alloy in the single nanoparticle bulk. Further degradation of the materials' magnetic properties can be associated with the decomposition of  $\text{Mn}_2\text{O}_3$  into  $\text{Mn}_3\text{O}_4$ .

Note that the formation of  $\text{Mn}_2\text{O}_3$  is not observed during the pure Mn-C composite calcination [24]. An important factor is the nanoparticles stability during annealing, in

contrast to the annealing of the Fe-C composite [20] at temperatures above 400°C, when the nanoparticles sinter into large agglomerates of more than 100 nm in size. High stability of the Fe-Mn-C nanocomposite during annealing made it possible to burn out most of the carbon without deteriorating the material magnetic properties and increasing the size of the nanoparticles. The proposed approach can be used to synthesize magnetic nanoparticles and nanofluids based on them.

#### 4. Conclusions

The phase composition and magnetic properties of nanoparticles formed during electric arc discharge with subsequent calcination of a composite Fe-Mn-C electrode were studied. The change dynamics of the Fe-Mn-C nanocomposite magnetic susceptibility during annealing comparing to Fe-C nanocomposite differs significantly. The presence of manganese in the system leads to the formation of  $\text{Mn}_x\text{Fe}_{3-x}\text{O}_4$  oxide and prevents the nanoparticles from sintering into large agglomerates. That, in turn, makes it possible to obtain nanocomposites with low carbon content. The magnetic susceptibility of such composites depends on their stoichiometry and ranges from  $\gamma\text{-Fe}_2\text{O}_3$  susceptibility value to FeC.

*Acknowledgements.* The study of materials by XRD was carried out under state contract with IT SB RAS, the study of TEM, magnetic properties and synthesis was financially supported by Russian Science Foundation (Project No. 18-19-00213P). The authors acknowledge the VTAN shared research facilities at NSU for the using the experimental equipment.

## References

1. M. Sheikholeslami, A. Shafee, A. Zareei, R.U. Haq, Z.Li. *Journal of Molecular Liquids*. 279, 719 (2019). [Crossref](#)
2. K. Zhou, X. Zhou, J. Liu, Z. Huang. *Journal of Petroleum Science and Engineering*. 188, 106943 (2020). [Crossref](#)
3. J.S. Beveridge, J.R. Stephens, M.E. Williams. *Annual Review of Analytical Chemistry*. 4, 251 (2011). [Crossref](#)
4. Q. A. Pankhurst, J. Connolly, S.K. Jones, J. Dobson. *Journal of physics D: Applied physics*. 36 (13), R167 (2003). [Crossref](#)
5. M. Namdeo, S. Saxena, R. Tankhiwale, M. Bajpai, Y.Á. Mohan, S.K. Bajpai. *Journal of Nanoscience and Nanotechnology*, 8 (7), 3247 (2008). [Crossref](#)
6. L.H. Reddy, J.L. Arias, J. Nicolas, P. Couvreur. *Chemical reviews*. 112 (11), 5818 (2012). [Crossref](#)
7. N. Löwa, J.M. Fabert, D. Gutkelch, H. Paysen, O. Kosch, F. Wiekhorst. *Journal of Magnetism and Magnetic Materials*. 469, 456 (2019). [Crossref](#)
8. J. Kudr, Y. Haddad, L. Richtera, Z. Heger, M. Cernak, V. Adam, O. Zitka. *Nanomaterials*. 7 (9), 243 (2017). [Crossref](#)
9. M. Bououdina, T.S. Alwqyan, L. Khezami, B. Al-Najar, M.N. Shaikh, R. Gill, O. M. Lemine. *Journal of Alloys and Compounds*. 772, 1030 (2019). [Crossref](#)
10. M. Hammad, S. Hardt, B. Mues, S. Salamon, J. Landers, I. Slabu, H. Wiggers. *Journal of Alloys and Compounds*. 824, 153814 (2020). [Crossref](#)
11. T.A. Shifa, F. Wang, Z. Cheng, P. He, Y. Liu, C. Jiang, J.He. *Advanced Functional Materials*. 28 (18), 1800548 (2018). [Crossref](#)
12. A.S. Lozhkomoev, O.V. Bakina, A.V. Pervikov, S.O. Kazantsev, E.A. Glazkova. *Journal of Materials Science: Materials in Electronics*. 30 (14), 13209 (2019). [Crossref](#)
13. N. Shatrova, A. Yudin, V. Levina, E. Dzidziguri, D. Kuznetsov, N. Perov, J.P. Issi. *Materials Research Bulletin*. 86, 80 (2017). [Crossref](#)
14. O.M. Darwesh, I.A. Matter, M.F. Eida. *Journal of Environmental Chemical Engineering*. 7 (1), 102805 (2019). [Crossref](#)
15. K. Gudikandula, S. Charya Maringanti. *Journal of Experimental Nanoscience*. 11 (9), 714 (2016). [Crossref](#)
16. S.D. Anderson, V.V. Gwenin, C.D. Gwenin. *Nanoscale research letters*. 14 (1), 1 (2019). [Crossref](#)
17. S. Dave, S. Dave, A. Mathur, J. Das. *Biological synthesis of magnetic nanoparticles*. In: *Nanobiotechnology*. Elsevier (2021) pp. 225 – 234. [Crossref](#)
18. S. Ahmadi, M. Fazilati, H. Nazem, S. M. Mousavi. *BioMed Research International*. 2021, 8822645 (2021). [Crossref](#)
19. A.I. Tsimmerman, I.I. Shanenkov, A.A. Sivkov, A.S. Ivashutenko, A.R. Nassyrbayev, V.A. Vlasov. *Bulletin of the Russian Academy of Sciences: Physics*. 86 (10), 1224 (2022). [Crossref](#)
20. S.A. Novopashin, M.A. Serebryakova, A.V. Zaikovskii. *Journal of Nanoscience and Technology*. 1, 13 (2015).
21. R. Ghosh Chaudhuri, S. Paria. *Chemical reviews*. 112 (4), 2373 (2012). [Crossref](#)
22. D.V. Smovzh, S.Z. Sakhapov, A.V. Zaikovskii, E.V. Boyko, O.A. Solnyshkina. *Vacuum*. 196, 110802 (2022). [Crossref](#)
23. Z.J. Zhang, Z.L. Wang, B.C. Chakoumakos, J.S. Yin. *Journal of the American Chemical Society*. 120 (8), 1800 (1998). [Crossref](#)
24. A.A. Iurchenkova, E.O. Fedorovskaya, P.E. Matochkin, S.Z. Sakhapov, D.V. Smovzh. *Int J Energy Res*. 44, 10754 (2020). [Crossref](#)
25. N. Dogan, O.M. Dogan, M. Irfan, F. Ozel, A.S. Kamzin, V.G. Semenov, I.V. Buryanenko. *Journal of Magnetism and Magnetic Materials*. 561, 169654 (2022). [Crossref](#)
26. H. Shao, C. Min, D. Issadore, M. Liong, T.J. Yoon, R. Weissleder, H.Lee. *Theranostics*. 2 (1), 55 (2012). [Crossref](#)
27. Y. Ma, X. Xu, L. Lu, K. Meng, Y. Wu, J. Chen, J. Miao, Y. Jiang. *Ceramics International*. 47 (24), 34005 (2021). [Crossref](#)
28. Y.W. Jun, J.H. Lee, J. Cheon. *Angewandte Chemie International Edition*. 47 (28), 5122 (2008). [Crossref](#)